

Finite-size version of the excitonic instability in graphene quantum dots

Tomi Paananen and Reinhold Egger

Institut für Theoretische Physik, Heinrich-Heine-Universität, D-40225 Düsseldorf, Germany

(Dated: November 22, 2021)

By a combination of Hartree-Fock simulations, exact diagonalization, and perturbative calculations, we investigate the ground-state properties of disorder-free circular quantum dots formed in a graphene monolayer. Taking the reference chemical potential at the Dirac point, we study $N \leq 15$ interacting particles, where the fine structure constant α parametrizes the Coulomb interaction. We explore three different models: (i) Sucher’s positive projection (“no-pair”) approach, (ii) a more general Hamiltonian conserving both N and the number of additional electron-hole pairs, and (iii) the full quantum electrodynamics (QED) problem, where only N is conserved. We find that electron-hole pair production is important for $\alpha \gtrsim 1$. This corresponds to a reconstruction of the filled Dirac sea and is a finite-size version of the bulk excitonic instability. We also address the effects of an orbital magnetic field.

PACS numbers: 03.65.Pm, 73.22.Pr, 71.15.Rf, 73.21.La

I. INTRODUCTION

Coulomb interaction effects in monolayer graphene^{1,2} are currently attracting a lot of attention; for a recent review, see Ref. 3. From a theory point of view, this interest mainly stems from the possibility of realizing a strong-coupling version of QED in a readily accessible two-dimensional (2D) system. In fact, the (bare) fine structure constant is rather large, $\alpha = e^2/(\hbar\kappa v_F) \simeq 2.2/\kappa$, with the effective substrate dielectric constant κ and the Fermi velocity $v_F \approx c/300 \approx 10^6$ m/s. Retardation effects are irrelevant here, i.e., we effectively have 2D massless Dirac fermions interacting via the Coulomb potential. Similar physics can be expected for the surface state in 3D topological insulators,⁴ but interactions are expected to be much weaker due to the large κ in the relevant materials. In graphene, the situation away from the Dirac point (defined as zero of energy) can be reasonably well understood in terms of Fermi liquid theory,^{3,5} but the picture is more complicated near the Dirac point. At a critical interaction strength α_c , a semimetal-insulator transition is theoretically expected⁶ due to electron-hole proliferation. For $\alpha > \alpha_c$, a finite gap corresponding to an excitonic insulator is formed and the ground state undergoes reconstruction. On the other hand, quantum critical behavior is expected^{7,8} as a precursor of the instability for $\alpha < \alpha_c$. Recent lattice quantum Monte Carlo simulations⁹ found the critical value $\alpha_c \approx 1.1$ for an infinitely extended (“bulk”) graphene monolayer. Similar values were also obtained analytically from the dynamical polarization function approach¹⁰ and under the ladder approximation to the Bethe-Salpeter equation.¹¹ However, so far no experimental signature of this *excitonic instability* has been reported. It has also been recognized that the excitonic instability for the bulk many-body problem is related to the simpler “supercritical” instability of the hydrogen problem in graphene,³ where α corresponds to the (attractive) potential strength of the nucleus. Above a critical value for α , the nucleus captures an electron to screen its positive charge below criti-

cality, while at the same time a hole escapes to infinity in order to maintain charge neutrality. In atomic physics, essentially the same phenomenon should also take place for superheavy atoms.¹² The creation of an electron-hole pair thus also accompanies the supercritical instability. In the presence of an homogeneous orbital magnetic field B , the hole escape process is disturbed by the formation of closed Landau orbits. For the bulk many-body problem, the resulting magnetic catalysis phenomenon¹³ implies a lowering of α_c with increasing B .

In this work, we study a finite-size version of the excitonic instability presumably realized in available graphene quantum dots. Quantum dots in conventional 2D systems have been studied extensively,^{14,15} and experimental results for lithographically prepared graphene dots were reported recently.^{16–20} Within the single-particle picture, theoretical proposals on how to model such a dot have been reviewed in Ref. 2. We here adopt the probably simplest route by imposing the so-called “infinite-mass boundary condition,”^{21,22} where no current is allowed to flow through the circle $r = R$ defining the dot’s boundary. While disorder limits the quality of the boundary in existing dots,²⁰ such a boundary condition captures at least their qualitative physics. Moreover, future experimental progress is likely to yield well-defined boundaries.

We investigate the ground state of N interacting electrons in a closed circular graphene dot, where N particles are added on top of the filled Dirac sea, i.e., relative to the chemical potential $\mu = 0$. This problem has been studied before within the Hartree-Fock (HF) approach.^{23–26} However, when going beyond effective single-particle theory, one has to deal with the “Brown-Ravenhall disease,”^{27,28} i.e., the possibility to excite electron-hole pairs with small energy by combining a hole and an electron both very far away from the Fermi surface. While such processes are physically suppressed by the finite bandwidth, the infinitely deep filled Dirac sea present in the Dirac theory renders naive approaches mathematically ill-defined. For $\alpha \ll 1$ and

when a gap separates electron and hole states, Sucher²⁸ showed that one can circumvent the Brown-Ravenhall problem by a suitable projection Λ_+ of the basic QED Hamiltonian H to a well-defined no-pair Hamiltonian $H_+ = \Lambda_+ H \Lambda_+$, where the filled Dirac sea is effectively treated as completely inert. The projection operator Λ_+ eliminates negative-energy (hole) states from the single-particle Hilbert space. We study the validity of the no-pair approach for graphene dots and find that for $\alpha \lesssim 1$, it is indeed meaningful, see also Ref. 29. On a quantitative level, however, it is accurate only for $\alpha \ll 1$. As also discussed by Sucher,²⁸ if one wishes to go beyond the positive projection scheme, a QED approach is indicated. The QED Hamiltonian H , see Eq. (11) below, does not conserve the number N_{eh} of electron-hole pairs. In fact, only the particle number N – defined as the imbalance of electron and hole numbers – is conserved, and a superposition of states with different N_{eh} determines the ground state for strong interactions. Once electron-hole pairs proliferate, a reconstruction of the ground state takes place. We encounter this phenomenon for $\alpha \gtrsim 1$ in graphene dots, similar to the reported critical value⁹ for the bulk excitonic instability. However, in our finite-size system this is a smooth crossover and not a phase transition. We stress that our “ N -particle problem” defines N as the difference of electron and hole numbers, which allows for the excitation of an arbitrary number N_{eh} of electron-hole pairs. For $\alpha \rightarrow 0$, this definition reduces to having N electrons on top of the filled Dirac sea.

The structure of the remainder of this paper is as follows. In Sec. II we introduce the model and discuss the various theoretical approaches employed to find the ground state. An intermediate approach is to generalize the no-pair approach (where $N_{eh} = 0$) to allow for a fixed but finite number N_{eh} of electron-hole pairs. The Hamiltonian H_{fix} is obtained from H by neglecting all terms that do not conserve N_{eh} . A sufficient (but not necessary) condition for the breakdown of the no-pair Hamiltonian H_+ arises when the ground-state energy of H_{fix} is lowered for some $N_{eh} > 0$. We assess the validity of the no-pair scheme in Sec. III by comparing to results obtained under H_{fix} and from the QED Hamiltonian H . We perform these calculations using exact diagonalization (ED) for $N = 2$ and $N = 3$ particles in the dot. In Sec. IV, we use H_+ to carry out detailed HF calculations for up to $N = 15$ particles and relatively weak interactions, $\alpha \leq 1$. We present results for the ground-state spin, valley polarization, and addition energy as function of N . Finally, in Sec. V we provide a discussion of our main results.

II. MODEL AND THEORETICAL APPROACHES

In this section, we describe the model employed in our study of the electronic properties of interacting graphene quantum dots. We will then turn to different theoretical

approaches to obtain the ground-state properties.

A. Single-particle problem

It is well established that on low energy scales, quasiparticles in graphene are described by the Dirac Hamiltonian,²

$$H_0 = v_F \boldsymbol{\sigma} \cdot \left(\mathbf{p} + \frac{e}{c} \mathbf{A} \right) + M(r) \sigma_z \tau_z - \mu_B \mathbf{s} \cdot \mathbf{B}, \quad (1)$$

where $\mathbf{p} = -i\hbar(\partial_x, \partial_y)^T$ and $-e$ is the electronic charge. The Pauli matrices $\boldsymbol{\sigma} = (\sigma_x, \sigma_y)$ and σ_z refer to graphene’s sublattice structure, while the Pauli matrix τ_z corresponds to the valley degree of freedom, i.e., to the two K points. A static vector potential $\mathbf{A}(\mathbf{r})$ [with $\mathbf{r} = (x, y)^T$] allows for the inclusion of a constant orbital magnetic field B_z , where we choose the symmetric gauge, $\mathbf{A} = \frac{1}{2} B_z (-y, x)^T$. Since we neglect spin-orbit couplings in Eq. (1), spin Pauli matrices $\mathbf{s} = (s_x, s_y, s_z)$ only appear in the Zeeman term. With μ_B denoting Bohr’s magneton and putting the Landé factor to $g_e = 2$,²⁰ this term couples to the full (homogeneous) magnetic field, $\mathbf{B} = (B_x, B_y, B_z)$ with $B = |\mathbf{B}|$. Switching to polar coordinates (r, ϕ) , we consider a clean circular quantum dot in a graphene monolayer modelled by the well-known infinite-mass boundary condition,²¹ where the mass $M(r)$ in Eq. (1) is zero for $r < R$ but tends to $+\infty$ for $r > R$. This choice ensures that no current flows through the boundary at $r = R$. Eigenstates can be classified by the conserved total angular momentum, $J_z = -i\hbar\partial_\phi + \hbar\sigma_z/2$, with eigenvalue $\hbar j$ for half-integer $j = m + 1/2$, $m \in \mathbb{Z}$.

While the eigenfunctions can be found in analytical form even in the presence of the magnetic field,²² the Coulomb interaction matrix elements are readily available²⁶ only in the $B = 0$ basis. We therefore first describe the solution for $B = 0$ and later include the homogeneous magnetic field. Note that different valleys ($\tau = \pm$) are decoupled and spin ($s = \pm$) then simply yields a twofold degeneracy. For given (m, τ, s) , we first discuss the $E > 0$ solutions to $H_0 \Phi^{(+)} = E \Phi^{(+)}$, where the spinor has the sublattice structure

$$\Phi^{(+)}(r, \phi) = e^{im\phi} \begin{pmatrix} \psi_{1,m}(r) \\ ie^{i\phi} \psi_{2,m}(r) \end{pmatrix}. \quad (2)$$

The infinite-mass boundary condition implies^{21,22}

$$\psi_{1,m}(R) = \tau \psi_{2,m}(R). \quad (3)$$

With the Bessel functions $J_m(kr)$ of the first kind, $k = E/\hbar v_F$, and normalization constant A , the Dirac equation for $r < R$ is solved by the *Ansatz*

$$\psi_{1,m}(r) = A J_m(kr), \quad \psi_{2,m} = A J_{m+1}(kr).$$

The quantization condition (3) then determines the eigenenergies $E_a > 0$ with $a \equiv (n, m, \tau, s)$,

$$J_m(E_a/\Delta_0) = \tau J_{m+1}(E_a/\Delta_0), \quad (4)$$

where $\Delta_0 \equiv \hbar v_F/R$ is the single-particle level spacing of the dot and $n \in \mathbb{N}$ labels different solutions for given (m, τ, s) . Equation (4) is easily solved numerically and the eigenstates to energy $E_a > 0$ are

$$\Phi_a^{(+)}(r, \phi) = A_a e^{im\phi} \begin{pmatrix} J_m(k_a r) \\ i e^{i\phi} J_{m+1}(k_a r) \end{pmatrix}, \quad (5)$$

where $k_a = E_a/\hbar v_F$ and the normalization factor is

$$A_a = [\pi(J_m^2 - J_{m-1}J_{m+1} + J_{m+1}^2 - J_mJ_{m+2})]^{-1/2} \quad (6)$$

with $J_m \equiv J_m(E_a/\Delta_0)$. Time-reversal invariance implies the Kramers degeneracy relation $E_{n,m,\tau,s} = E_{n,-m-1,-\tau,-s}$. Negative-energy (hole) solutions, $\Phi_{\tilde{a}}^{(-)}(r, \phi)$, follow by using the electron-hole symmetry property of the Hamiltonian, $E_{n,m,-\tau,s} = -E_{n,m,\tau,s}$. We use the multi-index a (\tilde{a}) to count states with positive (negative) energy. There is no zero-energy solution for $B = 0$, and we have a finite gap around the Dirac point.

Next we add the magnetic field. Expressed in terms of the eigenstates $\Phi_a^{(+)}$ and $\Phi_{\tilde{a}}^{(-)}$, the vector potential part in H_0 has a matrix structure diagonal both in the quantum numbers (m, τ, s) and the conduction/valence band index \pm , i.e., only different n states are mixed. By numerical diagonalization, it is straightforward to obtain the resulting eigenenergies $\tilde{E}_a > 0$ and $\tilde{E}_{\tilde{a}} < 0$, and the corresponding eigenstates. The indices n and thus a (\tilde{a}) are redefined to take into account the unitary transformation diagonalizing H_0 . Finally, we include the Zeeman term. Choosing the spin quantization axis along \mathbf{B} , where $s = \pm 1$ corresponds to spin-up or spin-down states, the full eigenenergy $E_a > 0$ is given by³⁰

$$E_a = \tilde{E}_a - s\mu_B B, \quad (7)$$

and similiary for $E_{\tilde{a}} < 0$. In a slight abuse of notation, E_a now denotes the full eigenenergy and not the solution to Eq. (4) anymore. The Zeeman term is generally quite small² but breaks the spin degeneracy of the levels, while the vector potential breaks the valley degeneracy, see Eq. (3). The resulting eigenstates are denoted by $\Phi_a^{(+)}(r, \phi)$ and $\Phi_{\tilde{a}}^{(-)}(r, \phi)$.

B. Many-body interactions

We now include the Coulomb interaction among the particles. The noninteracting reference problem is characterized by a filled Dirac sea ($\mu = 0$), i.e., all $E_{\tilde{a}} < 0$ states are filled. The QED Hamiltonian H describing this problem can be expressed in terms of electron annihilation operators, c_a , corresponding to the single-particle states $\Phi_a^{(+)}$, and hole creation operators, $d_{\tilde{a}}^\dagger$, with single-particle states $\Phi_{\tilde{a}}^{(-)}$. The full field operator is written as

$$\Psi(\mathbf{r}) = \sum_a \Phi_a^{(+)}(\mathbf{r})c_a + \sum_{\tilde{a}} \Phi_{\tilde{a}}^{(-)}(\mathbf{r})d_{\tilde{a}}^\dagger. \quad (8)$$

Since the Hamiltonian commutes with τ_z and $\mathbf{s} \cdot \mathbf{B}$, we can write $\Psi(\mathbf{r}) = \sum_{\tau s} \Psi_{\tau s}(\mathbf{r})$. The Hamiltonian is then

given by $H = H_k + H_I$, with the kinetic part (note that $E_{\tilde{a}} < 0$)

$$H_k = \sum_a E_a c_a^\dagger c_a + \sum_{\tilde{a}} |E_{\tilde{a}}| d_{\tilde{a}}^\dagger d_{\tilde{a}} \quad (9)$$

and the interaction term

$$H_I = \frac{\hbar v_F \alpha}{2} \sum_{\tau \tau' s s'} \int \frac{d\mathbf{r} d\mathbf{r}'}{|\mathbf{r} - \mathbf{r}'|} \times : \Psi_{\tau s}^\dagger(\mathbf{r}) \Psi_{\tau' s'}^\dagger(\mathbf{r}') \Psi_{\tau' s'}(\mathbf{r}') \Psi_{\tau s}(\mathbf{r}) :, \quad (10)$$

where the colons denote normal ordering. Inserting the field operator expansion (8) into Eq. (10),

$$H = H_{\text{fix}} + H'. \quad (11)$$

H_{fix} commutes separately with both the electron and the hole number operator, $\hat{N}_e = \sum_a c_a^\dagger c_a$ and $\hat{N}_h = \sum_{\tilde{a}} d_{\tilde{a}}^\dagger d_{\tilde{a}}$. The full Hamiltonian, however, only commutes with $\hat{N} = \hat{N}_e - \hat{N}_h$. We thus define the N -particle problem by having N excess electrons and $N_{eh} = N_h$ electron-hole pairs on top of the filled Dirac sea. Only N is conserved, while N_{eh} can fluctuate. Under H_{fix} alone, the number N_{eh} of electron-hole pairs is conserved,

$$H_{\text{fix}} = H_k + \frac{1}{2} \sum_{aba'b'} (V_{abb'a'} - \delta_{ss'} V_{aba'b'}) c_a^\dagger c_b^\dagger c_{b'} c_{a'} + \frac{1}{2} \sum_{\tilde{a}\tilde{b}\tilde{a}'\tilde{b}'} (V_{\tilde{a}\tilde{b}\tilde{a}'\tilde{b}'} - \delta_{ss'} V_{\tilde{a}\tilde{b}\tilde{a}'\tilde{b}'}) d_{\tilde{a}}^\dagger d_{\tilde{b}}^\dagger d_{\tilde{b}'} d_{\tilde{a}'} - \sum_{aa',\tilde{b}\tilde{b}'} (V_{a\tilde{b}\tilde{b}'a'} - \delta_{ss'} V_{a\tilde{b}\tilde{b}'a'}) c_a^\dagger d_{\tilde{b}}^\dagger d_{\tilde{b}'} c_{a'}. \quad (12)$$

All terms not commuting with $\hat{N}_{e,h}$ are collected in the remaining part, $H' = h + h^\dagger$, with

$$h = \frac{1}{2} \sum_{ab\tilde{a}'\tilde{b}'} (V_{ab\tilde{b}'\tilde{a}'} - \delta_{ss'} V_{ab\tilde{a}'\tilde{b}'}) c_a^\dagger c_b^\dagger d_{\tilde{b}'}^\dagger d_{\tilde{a}'}^\dagger + \frac{1}{2} \sum_{aa'\tilde{b}\tilde{b}'} \delta_{s,-s'} V_{a\tilde{b}\tilde{a}'\tilde{b}'} c_a^\dagger d_{\tilde{a}'}^\dagger d_{\tilde{b}'} c_{b'} + \sum_{abb'\tilde{a}'} (V_{abb'\tilde{a}'} - \delta_{ss'} V_{bab'\tilde{a}'}) c_a^\dagger d_{\tilde{a}'}^\dagger c_b^\dagger c_{b'} - \sum_{a\tilde{a}'\tilde{b}\tilde{b}'} (V_{a\tilde{b}\tilde{b}'\tilde{a}'} - \delta_{ss'} V_{a\tilde{b}\tilde{a}'\tilde{b}'}) c_a^\dagger d_{\tilde{a}'}^\dagger d_{\tilde{b}'}^\dagger d_{\tilde{b}'} c_{b'}. \quad (13)$$

In Eqs. (12) and (13), the spin quantum numbers are given by $s = s_a = s_{a'}$ and $s' = s_b = s_{b'}$ (when hole states are involved, $a \rightarrow \tilde{a}$ etc.). These spin selection rules are encoded in the interaction matrix elements $V_{aa'b'b}$ which have been derived in a form useful for numerical evaluation in Ref. 25. We quote them for the convenience of the reader next. A finite matrix element follows only when the valley selection rule, $\tau_a = \tau_{a'}$ and $\tau_b = \tau_{b'}$, and angular momentum conservation, $m_a + m_{a'} = m_b + m_{b'}$, are satisfied. When all selection rules are met,

$$\begin{aligned}
V_{aa'b'b} &= (4\pi)^2 \alpha \Delta_0 A_a A_{a'} A_{b'} A_b \sum_{l=0}^{\infty} C_{q,l} \int_0^1 dr r^{-l} (J_{m_a}(E_a r) J_{m_b}(E_b r) + J_{m_a+1}(E_a r) J_{m_b+1}(E_b r)) \\
&\times \int_0^r dr' (r')^{l+1} (J_{m_{a'}}(E_{a'} r') J_{m_{b'}}(E_{b'} r') + J_{m_{a'}+1}(E_{a'} r') J_{m_{b'}+1}(E_{b'} r')),
\end{aligned}$$

with E_a in units of $\Delta_0 = \hbar v_F/R$ and $q \equiv |m_b - m_a|$. The coefficient $C_{q,l}$ vanishes when $l+q$ is odd or when $l < q$. For $q = l = 0$, we have $C_{0,0} = 1/2$, while otherwise

$$C_{q,l} = \frac{(2l-1)!!}{2^{l+1}l!} \prod_{n=1}^{(l+q)/2} \frac{(n-1/2)(n-l-1)}{n(n-l-1/2)}.$$

C. Calculation approaches

A standard way to proceed is to employ the no-pair approach.²⁶ With the projector Λ_+ to the subsector $E_a > 0$ of the single-particle Hilbert space (for each particle), we thus consider the N -particle problem with respect to the filled Dirac sea. The projected Hamiltonian $H_+ = \Lambda_+ H \Lambda_+ = \Lambda_+ H_{\text{fix}} \Lambda_+$ is given by

$$\begin{aligned}
H_+ &= \sum_a E_a c_a^\dagger c_a \\
&+ \frac{1}{2} \sum_{aba'b'} (V_{abb'a'} - \delta_{ss'} V_{aba'b'}) c_a^\dagger c_b^\dagger c_{b'} c_{a'}.
\end{aligned} \tag{14}$$

As detailed in Refs. 25,26, this allows for a straightforward implementation of the HF approach, and we will report HF results in Sec. IV. In contrast to Refs. 25,26, we here include the valley and spin degrees of freedom. Given the converged self-consistent density matrix, one can obtain the ground-state energy $E(N)$, the total spin quantum number S of the N -electron dot from the eigenvalues $\hbar^2 S(S+1)$ of $\sum_{i=1}^N \mathbf{S}_i^2$, and the valley polarization eigenvalue $\tau(N) = \sum_i \tau_i$.

On a more general level, we allow for a fixed number of electron-hole pairs by employing the Hamiltonian H_{fix} [Eq. (12)]. The no-pair Hamiltonian H_+ follows from H_{fix} with $N_{eh} = 0$. When the ground-state energy of H_{fix} is minimized for some $N_{eh} > 0$, the no-pair approach breaks down. Interactions are then able to overcome the gap between valence and conduction band, and one cannot treat the Dirac sea as inert anymore. H_{fix} as well as the QED model H are studied by ED and perturbation theory in Sec. III.

III. PARTICLE-HOLE PAIR PRODUCTION AND RECONSTRUCTION OF THE GROUND STATE

We now compare the three theoretical approaches in Sec. II C by employing ED for particle numbers $N = 2$

Γ

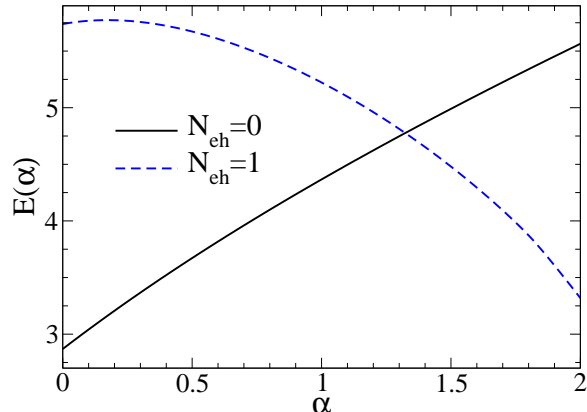


FIG. 1: (Color online) ED results for the ground-state energy E in units of $\Delta_0 = \hbar v_F/R$ vs fine structure constant α for $N = 2$ particles in a graphene dot with $B = 0$. We here use the Hamiltonian H_{fix} in Eq. (12).

and 3. Convergence in the ED calculations was achieved by keeping about 30 single-particle states (per spin and valley degree of freedom), and memory size limitations represented the main bottleneck. For a given α , ED results can be obtained within a few minutes on a standard desktop computer.

Figure 1 shows results for the α -dependence of the ground-state energy for $N = 2$ using H_{fix} with $N_{eh} = 0$ and 1. We observe that for $\alpha \lesssim 1.3$, the ground state of H_{fix} contains no electron-hole pair, but for stronger interaction, the ground state undergoes reconstruction and involves at least one electron-hole pair. The no-pair Hamiltonian H_+ thus necessarily fails when $\alpha \gtrsim 1.3$. Moreover, as we shall discuss next, the presence of H' [Eq. (13)] restricts its applicability even further.

Since ED of the QED Hamiltonian H in Eq. (11) is computationally very demanding even for $N = 2$, in the remainder of this section, we shall restrict ourselves to a spinless single-valley version of graphene. The ED results obtained from H_{fix} and H are compared for $N = 2$ in Fig. 2. For the spinless single-valley version of H_{fix} , no electron-hole pairs are excited in the ground state for $\alpha \lesssim 1.9$. However, the H' contribution is important already for $\alpha \gtrsim 0.5$, see Fig. 2. The full interaction correction to the energy is significantly lowered by including H' and may even change sign for large α . In these calculations, the Hilbert space was truncated to contain at most one

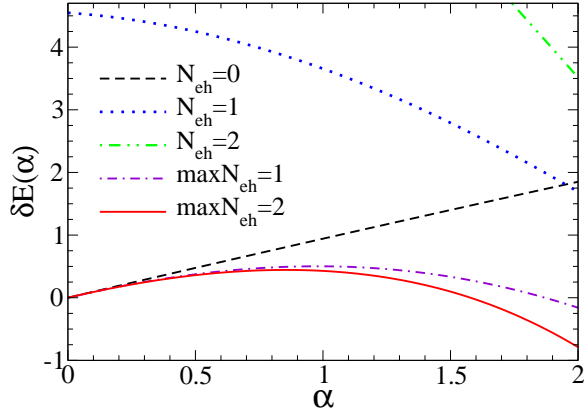


FIG. 2: (Color online) ED results for the interaction energy $\delta E(\alpha) = E(\alpha) - E(0)$ (in units of Δ_0) vs α for $N = 2$. We consider a spinless single-valley version of graphene with $B = 0$. The curves for $N_{eh} = 0, 1, 2$ correspond to the Hamiltonian H_{fix} with N_{eh} electron-hole pairs, i.e., the ground state then has no electron-hole pair for $\alpha \lesssim 1.9$. However, the full QED Hamiltonian (11), where we truncate the Hilbert space to at most one or two electron-hole pairs ($\max(N_{eh}) = 1, 2$), has a significantly lower energy already for $\alpha \gtrsim 0.5$.

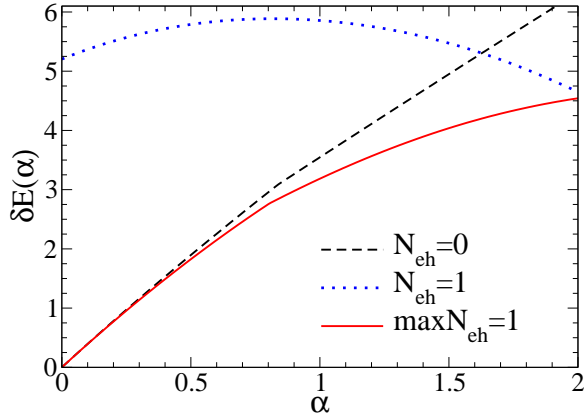


FIG. 3: (Color online) Same as Fig. 2 but for $N = 3$.

or two electron-hole pairs. For $\alpha \lesssim 1.5$, this appears to be sufficient. Figure 3 shows results for $N = 3$, where we arrive at similar conclusions.

The effect of H' can also be evaluated analytically by using second-order perturbation theory (the first order vanishes identically). The result is shown for $N = 2$ in Fig. 4, together with the ED results from Fig. 2. We see that second-order perturbation theory captures the ED data quite well, especially for $\alpha \lesssim 1$. The same conclusion was reached for $N = 3$ (results not shown here), and the combination of ED (or HF) calculations for H_{fix} supplemented with a perturbative treatment of H' should in general provide a good approximation of the ground state.

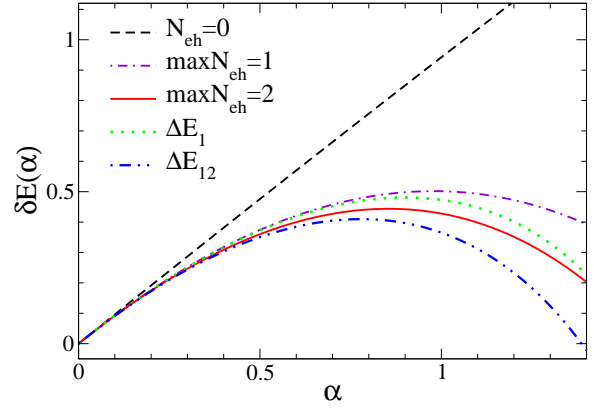


FIG. 4: (Color online) Same as Fig. 2 but including the results of second-order perturbation theory in H' . The curve ΔE_1 takes into account corrections involving one electron-hole pair only, while ΔE_{12} is the full second-order result including up to two pairs.

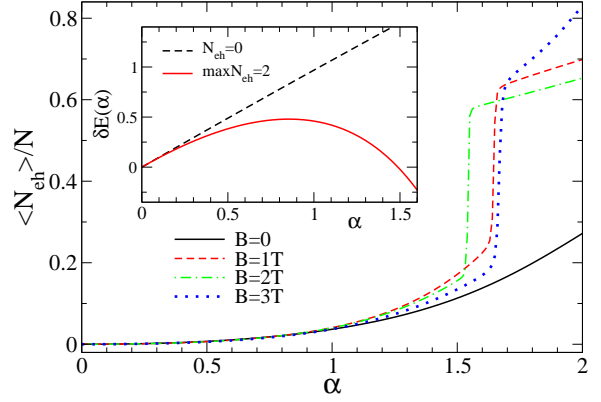


FIG. 5: (Color online) Main panel: Relative number of electron-hole pairs in the ground state, $\langle N_{eh} \rangle / N$, vs α for $N = 2$ and several values of the magnetic field. We take the dot radius $R = 30$ nm. The results were obtained using the QED Hamiltonian but with the Hilbert space truncated to at most two electron-hole pairs. Inset: Interaction correction δE vs α for $N = 2$ and $B = 1$ T. Shown are ED results using H_+ ($N_{eh} = 0$) and for the full H , where the Hilbert space was truncated at $\max(N_{eh}) = 2$.

Let us now discuss the case of finite magnetic field, again for the computationally simpler spinless single-valley case with $N = 2$. We have also studied $N = 3$ particles, again with very similar results. The main panel of Fig. 5 shows the average number of electron-hole pair excitations in the ground state for several values of the magnetic field. The shown results are for a dot radius $R = 30$ nm. A magnetic field of $B = 1$ T corresponds to the magnetic length $l_B = (c/eB)^{1/2} \approx 26$ nm, which is of the same order of magnitude as the radius. Evidently, in a magnetic field, the proliferation of electron-

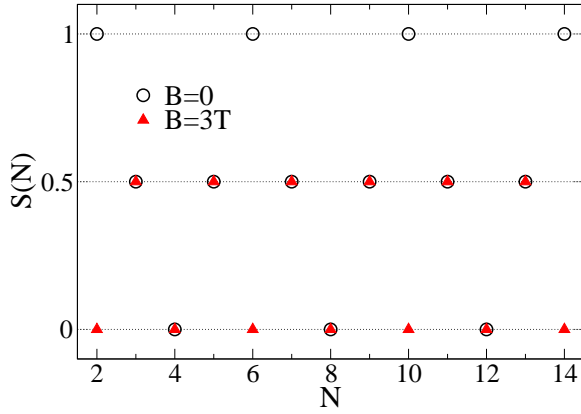


FIG. 6: (Color online) HF results using the no-pair model, H_+ , for the ground-state spin S vs particle number N for $B = 0$ and for $B = B_z = 3$ T (with $R = 30$ nm). For all shown N and $\alpha \leq 1$, $S(N)$ does not depend on α .

hole pairs becomes more important. We interpret this effect as the finite-size analogue of the magnetic catalysis phenomenon.¹³ The interaction correction to the ground-state energy is shown for $B = 1$ T in the inset of Fig. 5. While the result shows qualitatively similar behavior as for $B = 0$, the now more significant deviations between the ED data and the no-pair result are consistent with magnetic catalysis again. We note in passing that for $\alpha \gtrsim 1.5$, the basis size used in our ED calculations is most likely not sufficient, and probably $N_{eh} > 2$ states also contribute to the ground state. The steplike features in Fig. 5 are then presumably smeared out.

We conclude that the no-pair Hamiltonian is quantitatively reliable only for weak interactions, $\alpha \lesssim 0.5$, and for not too large magnetic fields. For stronger interactions and/or fields, the ground state undergoes reconstruction and electron-hole pair proliferation. Using H_{fix} [Eq. (12)] is not sufficient to get more accurate results, and one has to include H' [Eq. (13)] which does *not* conserve the electron and hole numbers separately. However, for $\alpha \lesssim 1$, quite accurate results for the ground-state energy are obtained by combining ED (or HF) calculations for the no-pair Hamiltonian with subsequent second-order perturbation theory in H' . Here only two or three particles have been addressed, where electron-hole proliferation takes place around $\alpha \approx 1$. Since the bulk case, which follows from the above model by a suitable limiting procedure with $N \rightarrow \infty$ and $R \rightarrow \infty$, has a phase transition at $\alpha \approx 1.1$, the finite-size crossover apparently depends on N only weakly.

IV. ADDITION SPECTRUM AND GROUND-STATE PROPERTIES

Let us now turn to HF results for the ground state of the N -electron dot with $N \leq 15$ using the no-pair

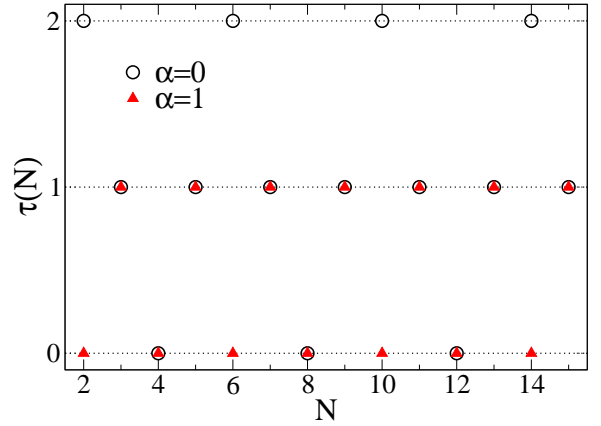


FIG. 7: (Color online) HF results for the ground-state valley polarization $\tau(N) = \sum_{i=1}^N \tau_i$ in the zero-field case with $\alpha = 0$ and $\alpha = 1$. For $\alpha = 0.5$, the same result as for $\alpha = 1$ is found.

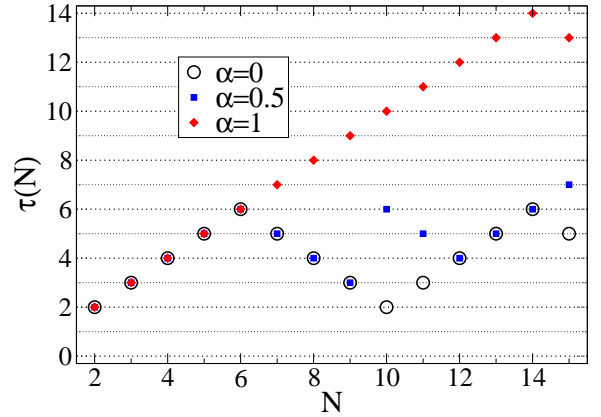


FIG. 8: (Color online) Same as Fig. 7 but for a perpendicular magnetic field with $B = 3$ T (with $R = 30$ nm).

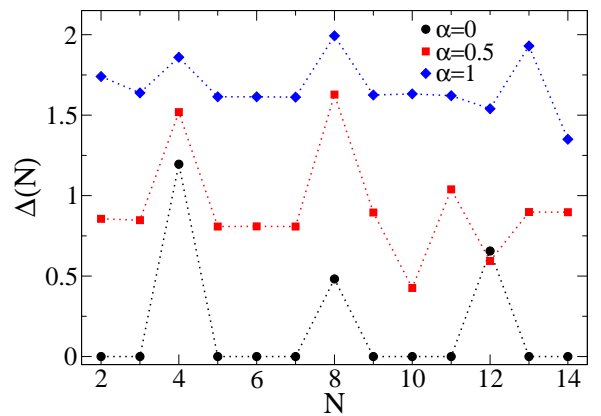


FIG. 9: (Color online) Addition energy (15) in units of Δ_0 vs N for several α from HF calculations for H_+ with $B = 0$.

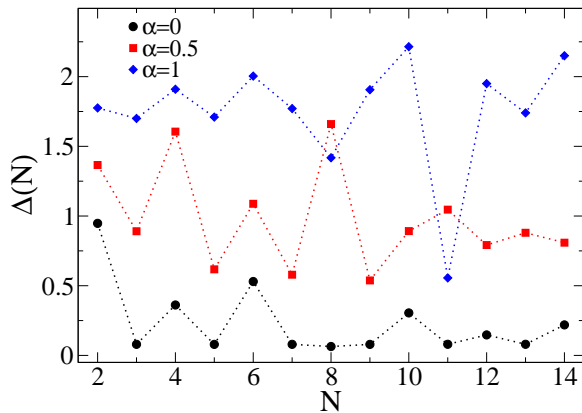


FIG. 10: (Color online) Same as Fig. 9 but with $B_x = 15$ T and $B_z = 3$ T (for $R = 30$ nm).

Hamiltonian H_+ [Eq. (14)]. As discussed in Sec. III, this approximation is reliable only for weak interactions, and we focus on the regime $\alpha \leq 1$ below. The spin and valley degrees of freedom are fully included in our self-consistent HF calculations.

The total ground-state spin S follows from the eigenvalue $\hbar^2 S(S+1)$ of the total squared spin operator and is shown as a function of N in Fig. 6, both for $B = 0$ and in the perpendicular magnetic field $B = 3$ T. For $N \leq 14$ and $\alpha \leq 1$, the spin filling sequence $S(N)$ is independent of the interaction strength α and displays a four-periodicity for $B = 0$. For $B \neq 0$, this periodicity is reduced to a two-periodicity since now spin degeneracy is broken. We note that the spin filling sequence can be measured experimentally by Coulomb blockade spectroscopy.²⁰

The total ground-state valley polarization, $\tau(N)$, is shown in Fig. 7 for $B = 0$, and in Fig. 8 under the perpendicular field $B = 3$ T. When $B = 0$, the full Hamiltonian is symmetric under $\tau \rightarrow -\tau$, and we here show only the positive solution. However, a finite orbital field B lifts the valley degeneracy. We observe from Fig. 7 that for $B = 0$, interactions reduce the four-periodicity of $\tau(N)$ for $\alpha = 0$ down to a two-periodicity. This can be understood by noting that the interaction of particles in different valleys is typically weaker than the intra-valley interaction. For $B \neq 0$, this implies pronounced interaction effects on the valley polarization. Figure 8 shows that strong interactions force subsequent particles to be added into the same valley, thereby valley-polarizing the N -particle system. Both the spin and valley filling sequences obtained by HF theory have been independently confirmed by ED of the no-pair Hamiltonian for $N \leq 4$ (data not shown).

To estimate the accuracy of the HF approximation for the no-pair model, we have also determined the relative difference between the HF (E_{HF}) and the ED (E_{ED}) en-

ergy,

$$\delta(N) = \frac{E_{\text{HF}}(N, \alpha) - E_{\text{ED}}(N, \alpha)}{E_{\text{ED}}(N, \alpha) - E_{\text{ED}}(N, 0)}.$$

In all studied cases ($N \leq 4$), $\delta(N)$ was found to be rather small. For instance, even when taking the large value $\alpha = 1.5$, we obtain $\delta(2) = 0.107$, $\delta(3) = 0.175$ and $\delta(4) = 0.148$. As long as the no-pair approach stays valid, we conclude that HF theory yields quite accurate results.

Our HF results for the *addition energy*,¹⁵ which follows from the ground-state energy $E(N)$ using the relation

$$\Delta(N) = E(N+1) + E(N-1) - 2E(N), \quad (15)$$

are shown in Fig. 9 for $B = 0$ and several α . (Similar HF results but for the spinless single-channel version were discussed in Ref. 26.) Peaks in $\Delta(N)$ signify especially stable dot configurations (magic numbers). While for $\alpha = 0$, $\Delta(N)$ again shows the four-periodicity due to spin-valley degeneracy, the addition energy peaks become less pronounced with interactions, and the four-periodicity is not always visible. Interestingly, while there are magic numbers $N = 4, 8, 12, \dots$ related to completely filled “energy shells” in the noninteracting case, the addition energy curves $\Delta(N)$ are rather featureless and almost flat for strong interactions. This indicates that a constant interaction model³² provides a reasonable description, where the microscopic Coulomb interaction is replaced by the electrostatic charging energy of an effective capacitor. The addition energy $\Delta(N)$ for $B \neq 0$ is shown in Fig. 10. The in-plane part B_x of the magnetic field here acts to increase the spin Zeeman field. However, Zeeman effects in graphene are weak,² and indeed almost the same results as those in Fig. 10 were found for $B_x = 0$ and $B_z = 3$ T. As a consequence of the broken spin degeneracy, only an (approximate) two-periodicity in $\Delta(N)$ is observed in the magnetic field case.

V. CONCLUSIONS

In this work, we have studied the ground state properties of N particles in a disorder-free circular graphene quantum dot, with the filled Dirac sea as the point of reference. The boundary of the dot has been modelled by the infinite-mass boundary condition, and the particles interact via the unscreened Coulomb potential whose prefactor is proportional to the bare dimensionless fine structure constant α . In contrast to atomic physics where $\alpha = 1/137$ is very small, in graphene (e.g., by the variation of the substrate dielectric parameter) α may be tuned up to a maximum value of $\alpha \approx 2.2$ (reached for freely suspended samples). For instance, a recent experiment²⁰ using Coulomb blockade spectroscopy for a graphene dot reported $\alpha \approx 1$. We have studied the N -particle problem in a graphene dot on various levels of complexity – from the no-pair Hamiltonian to the full QED model – and by a number of different techniques. Our main results are as follows.

By using exact diagonalization (ED) for $N = 2$ and 3 particles, we found that the no-pair Hamiltonian H_+ originally proposed by Sucher,²⁸ where the filled Dirac sea is assumed to be inert, is quantitatively reliable only for $\alpha \ll 1$, see Sec. III. While this represents the standard situation in atomic physics,³¹ it can easily be violated in graphene. For $\alpha \gtrsim 0.5$, our calculations indicate that electron-hole pair excitations contribute to the ground state energy. For $\alpha \gtrsim 1$, these excitations proliferate and eventually cause a completely restructured ground state. Technically, the projection operator Λ_+ defining the vacuum should thus be changed to include interaction effects in a self-consistent manner. Mittleman³³ has shown that this goal can be achieved by first minimizing the ground state energy $E(N, \Lambda_+)$ for given Λ_+ , followed by the maximization of the energy over all possible Λ_+ . The final result for $E(N)$ should then be equivalent to the QED results obtained numerically by ED (in the limit of infinite basis size).

We here argue that graphene dots realize a finite-size crossover version of the bulk semimetal-insulator phase transition. We find that the crossover scale is set by $\alpha \approx 1$, consistent with the bulk result $\alpha_c \approx 1.1$.⁹ When an orbital magnetic field is applied – the Zeeman field plays no significant role – electron-hole pair proliferation sets in earlier and implies a lowering of α_c , consistent with the magnetic catalysis scenario.¹³ Even on a qualitative level, the no-pair Hamiltonian H_+ is thus reliable only on the semimetallic side of the transition ($\alpha \lesssim 1$).

For the regime $\alpha \leq 1$, we have reported detailed results using Hartree-Fock theory for H_+ and $N \leq 15$ particles in Sec. IV, taking into account the spin and valley de-

grees of freedom. We find a four- (two-)periodicity in the spin filling sequence in the absence (presence) of a magnetic field, which can be understood from the single-particle picture and remains unaffected by weak interactions. However, the valley filling sequence is more intricate, especially when $B \neq 0$. This is related to subtle differences between the intra- and inter-valley scattering matrix elements of the Coulomb interaction. We observe a strong tendency towards valley polarization induced by interactions in this N -body problem. Finally, our analysis of the addition energy spectrum reveals that the constant interaction model can provide a reasonable description.

In our previous HF study of the spinless single-valley no-pair problem,²⁶ we found that Wigner molecule formation sets in for strong interactions. Since that regime corresponds precisely to the onset of electron-hole proliferation, $\alpha \gtrsim 1$, where the no-pair model becomes unreliable, we have analyzed the question of Wigner molecule formation using ED for $N = 3$ under the full QED model again. The Wigner molecule is identified from pronounced density correlations, and our numerical results (not shown here) are very similar to what we reported in Ref. 26. We thus expect that the Wigner molecule formation is only weakly affected by the electron-hole pair proliferation reported in this paper.

Acknowledgments

We thank A. De Martino, H. Siedentop and E. Stockmeyer for discussions. This work was supported by the SFB TR 12 of the DFG.

-
- ¹ A.K. Geim and K.S. Novoselov, *Nature Materials* **6**, 183 (2007).
- ² A.H. Castro Neto, F. Guinea, N.M.R. Peres, K.S. Novoselov, and A. Geim, *Rev. Mod. Phys.* **81**, 109 (2009).
- ³ V.N. Kotov, B. Uchoa, V.M. Pereira, A.H. Castro Neto, and F. Guinea, *Rev. Mod. Phys.* (in press); arXiv:1012.3484.
- ⁴ M.Z. Hasan and C.L. Kane, *Rev. Mod. Phys.* **82**, 3045 (2010).
- ⁵ J. González, F. Guinea, and M.A.H. Vozmediano, *Phys. Rev. B* **63**, 134421 (2001).
- ⁶ D.V. Khveshchenko, *J. Phys.: Cond. Matt.* **21**, 075303 (2009).
- ⁷ D.T. Son, *Phys. Rev. B* **75**, 235423 (2007).
- ⁸ M. Müller, J. Schmalian, and L. Fritz, *Phys. Rev. Lett.* **103**, 025301 (2009).
- ⁹ J.E. Drut and T.A. Lähde, *Phys. Rev. Lett.* **102**, 026802 (2009); *Phys. Rev. B* **79**, 165425 (2009).
- ¹⁰ O.V. Gamayun, E.V. Gorbar, and V.P. Gusynin, *Phys. Rev. B* **81**, 075429 (2010); *Phys. Rev. B* **83**, 235104 (2011).
- ¹¹ J. Wang, H.A. Fertig, G. Murthy, and L. Brey, *Phys. Rev. B* **83**, 035404 (2011).
- ¹² W. Greiner, B. Müller, and J. Rafelski, *Quantum electrodynamics of strong fields* (Springer, Berlin, 1985).
- ¹³ V.P. Gusynin, V.A. Miransky, and I.A. Shovkovy, *Phys. Rev. Lett.* **73**, 3499 (1994).
- ¹⁴ L.P. Kouwenhoven, D.G. Austing, and S. Tarucha, *Rep. Prog. Phys.* **64**, 701 (2001).
- ¹⁵ S.M. Reimann and M. Manninen, *Rev. Mod. Phys.* **74**, 1283 (2002).
- ¹⁶ L.A. Ponomarenko, F. Schedin, M.I. Katsnelson, R. Yang, E.W. Hill, K.S. Novoselov, and A.K. Geim, *Science* **320**, 356 (2008).
- ¹⁷ K. Todd, H.T. Chou, S. Amasha, and D. Goldhaber-Gordon, *Nano Lett.* **9**, 416 (2009).
- ¹⁸ K.A. Ritter and J.W. Lyding, *Nature Materials* **8**, 235 (2009).
- ¹⁹ J. Güttinger, C. Stampfer, F. Libisch, T. Frey, J. Burgdorfer, T. Ihn, and K. Ensslin, *Phys. Rev. Lett.* **103**, 046810 (2009).
- ²⁰ J. Güttinger, T. Frey, C. Stampfer, T. Ihn, and K. Ensslin, *Phys. Rev. Lett.* **105**, 116801 (2010).
- ²¹ M.V. Berry and R.J. Mondragon, *Proc. R. Soc. Lond. A* **412**, 53 (1987).
- ²² S. Schnez, K. Ensslin, M. Sigrüst, and T. Ihn, *Phys. Rev. B* **78**, 195427 (2008).
- ²³ B. Wunsch, T. Stauber, and F. Guinea, *Phys. Rev. B* **77**, 035316 (2008).

- ²⁴ M. Ezawa, Phys. Rev. B **77**, 155411 (2008).
- ²⁵ R. Egger, A. De Martino, H. Siedentop, and E. Stockmeyer, J. Phys. A: Math. Theor. **43**, 215202 (2010).
- ²⁶ T. Paananen, R. Egger, and H. Siedentop, Phys. Rev. B **83**, 085409 (2011).
- ²⁷ G.E. Brown and D.G. Ravenhall, Proc. R. Soc. London Ser. A **208**, 552 (1951).
- ²⁸ J. Sucher, Phys. Rev. **107**, 1448 (1957); Phys. Rev. **109**, 1010 (1958); Phys. Rev. A **22**, 348 (1980); Int. J. Quantum Chem. **25**, 3 (1984).
- ²⁹ W. Häusler and R. Egger, Phys. Rev. B **80**, 161402(R) (2009).
- ³⁰ In the HF calculations, it is sometimes advantageous to include a small mixing term in the single-particle Hamiltonian, $H_{\text{mix}} = \delta_K \tau_x + \delta_s s_x$. Inclusion of H_{mix} in the construction of the eigen-energies and -states is straightforward. This allows us to probe all spin and valley states in one run, and by careful extrapolation $\delta_K, \delta_s \rightarrow 0$, we can extract the ground state.
- ³¹ M. Reiher and A. Wolf, *Relativistic quantum chemistry* (Wiley VCH, Weinheim, 2009).
- ³² H. Grabert and M.H. Devoret (eds.), *Single Charge Tunneling*, NATO ASI Series B, Physics v.294 (Plenum Press, New York, 1992).
- ³³ M.H. Mittleman, Phys. Rev. A **24**, 1167 (1981).